Dasatinib loaded nanostructured lipid carriers for effective treatment of corneal neovascularization

Qingqing Li
Xi'an Jiaotong University
Xianwei Yang
Xi'an Jiaotong University
Peipei Zhang
Xi'an Jiaotong University
Fei Mo
Xi'an Jiaotong University
Peiru Si
Xi'an Jiaotong University
Ximeng Kang
Xi'an Jiaotong University
Menghan Wang
Xi'an Jiaotong University
Jiye Zhang (zjy2011@mail.xjtu.edu.cn)
Xi'an Jiaotong University https://orcid.org/0000-0003-4200-7043

Research

Keywords: Corneal neovascularization, Nanostructured lipid carriers, Dasatinib, Src family kinase

Posted Date: June 23rd, 2020

DOI: https://doi.org/10.21203/rs.3.rs-36557/v1

Version of Record: A version of this preprint was published at Biomaterials Science on January 1st, 2021.
See the published version at https://doi.org/10.1039/D0BM01599G.

Abstract

Corneal neovasularization (CNV) is one of the most important causes of visual impairment worldwide. Dasatinib, a poorly water-soluble tyrosine kinase inhibitor with dual Src family kinase and platelet derived growth factor receptor inhibiting capability, has a great potential in the treatment of CNV. In this study, dasatinib was successfully encapsulated into a nanostructured lipid carrier (dasa-NLC) and the size was approximately 78 nm with a small polydispersity index. The NLC increased the solubility of dasatinib by more than 1220 times, sustained the drug release, reduced the ocular toxicity and facilitated its penetration into the cornea. Dasa-NLC significantly inhibited the proliferation, migration and tube formation of HUVEC cells, the three most important angiogenesis-related cellular changes of the CNV. Next, the in vivo anti-CNV effect of dasa-NLC was evaluated by using an alkaline burned mice CNV model, in which the development of the CNV and pathological changes of the cornea were significantly inhibited. The immunohistochemistry analysis indicated that dasa-NLC could inhibit both the expression and activation of Src family kinase. Therefore, dasa-NLC showed considerable promise in the treatment of CNV.

1. Introduction

The transparency and avascularity of the cornea are essential to preserve the proper visual function. A wide variety of ocular insults, such as infection, inflammation, trauma, contact lens wear related hypoxia *et, al.*,(1) could result in abnormal angiogenesis in the cornea, namely, cornea neovascularization (CNV). The physical presence of the vessels not only blocks and diffracts light, but also leads to the deposition of lipids and proteins in the stroma layer of the cornea, impairs the structural integrity of the cornea(2, 3). CNV is the second cause of severe visual impairment worldwide. The incidence rate of CNV is estimated to be 1.4 million people per year, among them, 12% suffers subsequent vision loss(2). It is also the leading factor for corneal transplantation rejection(4). However, the anti-CNV therapies nowadays are mainly off-label corticosteroids and anti-angiogenic agents. There is no approved pharmacological treatment specific for CNV(1), therefore highly efficacious therapies with good ocular compatibility is in urgent needs.

The progress of angiogenesis involves vessel destabilization, endothelial cell activation, proliferation, migration, immature vessel formation, mural cells and matrix deposition and vessel maturation(5). Various growth factors such as vascular endothelial growth factor (VEGF), basic fibroblast growth factor (bFGF), platelet derived growth factor (PDGF), *etc.* are reported to be involved in the regulation of angiogenesis(5, 6). Src family kinase is a key component in the angiogenic signaling cascades activated by these growth factors and its downstream signaling pathway includes PI3K, FAK, ERK et, al., which play crucial roles in the neovascularization process(7, 8). Dasatinib is a tyrosine kinase inhibitor with dual PDGFR and Src family kinase inhibiting effect(9). Thus, attenuating angiogenesis with dasatinib may be a sound therapeutic strategy for CNV.

Besides drug selection, drug delivery challenges should also be considered for ocular diseases. Drug molecules with good *in vitro* efficacy may turn out to be inefficacious *in vivo* due to the inefficient and insufficient ophthalmic delivery. Eye drop is the most convenient and widely accepted dosage form for ocular diseases, especially for diseases in ocular surface. However, the delivery efficiency in the anterior segment of the eye is generally quite low due to limited administration volume and fast drug clearance from the cul-de-sac(10). Typically, ≤ 1% of a topically applied dose is estimated to enter the eye(11). Therefore, delivery systems which can enhance the solubility, sustain the drug release and facilitate the penetration of drugs into the cornea are highly desired to maximize the drug delivery efficiency and minimize the ocular toxicity at the same time. As the second generation of solid lipid nanoparticles, nanostructured lipid carrier (NLC) has gained lots of interests as an ocular drug delivery system due to its good ocular compatibility, enhanced ocular bioavailability, sustained drug release properties, *etc.*(4, 12–14) Therefore, in this study we sought to assess the potential of dasatinib loaded NLC (dasa-NLC) in the management of CNV. We aimed to: fabricate and physically characterize dasa-NLC; evaluate its *in vitro* anti-CNV efficacy via several angiogenesis related cell-based assays; examine its ocular safety and *in vivo* anti-CNV efficacy. Our research is the first systematic study in exploring the therapeutic potential of dasa-NLC for the inhibition of CNV.

2. Materials And Methods

2.1. Materials

Dasatinib, glyceryl monosterate, lipopolysaccharides and sodium fluorescein were purchased from Aladdin® (Shanghai, China). Coumarin-6 was obtained from TCI Co., Ltd. (Tokyo, Japan). Gelucire 44/14, Miglyol 812 N, Solutol® HS15 were gifts from Gattefosse (Paris, France), Sasol (Witten, Germany) and BASF (Lud-wigshafen, Germany), respectively. Soy lecithin and parafomaldehyde were obtained from Kemiou Chemical Reagent Co., (Tianjin, China). Matrigel® Matrix and dialysis bag (molecular cutoff of 3500 KD) were bought from Corning and Biosharp (USA), respectively. Anti-Src rabbit polyclonal antibody and HRP conjugated Goat Anti-mouse IgG (H + L) were purchased from Servicebio Ltd., (Wuhan, China). Anti-Src phospho Y418 antibody was acquired from abcam (Cambridge, UK). All chemicals used in this study were of analytical grade or better.

2.2 Animals

Ocular damage free New Zealand albino rabbits (male, 2.0-2.5 kg) and Balbc mice (male, 6 to 8 weeks old) were purchased from Laboratory Animal Service Center in the Xi'an Jiaotong University. All animal experiment procedures were approved by the Institutional Animal Ethical Committee of the Xi'an Jiaotong University.

2.3. Methods

2.3.1. Preparation of dasa-NLC

Dasa-NLC was prepared by a melt-emulsification method reported before with modification(15). Briefly, 275 mg of the lipid phase (5 mg dasatinib, 112 mg glycerin monosterate, 69 mg Miglyol 812 N and 89 mg Solutol®HS 15) and 10 mL of the aqueous phase (3 mg/mL Gelucire 44/14 and 3 mg/mL soy lecithin) was heated in a water bath of 75 °C. Next, the aqueous phase was dropwise added into the lipid phase under magnetic stirring. 5 min later, the mixed solution was homogenized for 15 min before being rapidly cooled in an ice bath. The sample was subsequently centrifuged for 5 min at 15000 rpm followed by being filtered by a 0.22 μm filter to remove the unencapsulated drug. Blank and coumarin 6-loaded NLC (coumarin 6-NLC) were prepared in the same manner.

2.3.2. Characterization of dasa-NLC

2.3.2.1. Particle size analysis

The average particle size, polydispersity index (PDI) and zeta potential of dasa-NLC were analyzed by a Zeta-sizer Nano (Malvern Instruments, UK).

2.3.2.2. Encapsulation efficiency

The encapsulation efficiency (EE%) and drug loading (DL%) of the dasa-NLC were determined by an HPLC. HPLC conditions were as follows: a XTerrra RP C18 column (150 mm × 4.6 mm, 5 μm, Waters) was used. The mobile phase was a mixture of acetonitrile and 0.1% formic acid (95:5, v/v). The flow rate was 1.0 mL/min and the column temperature was 25 °C. The detection wavelength was set as 323 nm. EE% and DL% were calculated with the following formula:

$$\mathrm{DL}\,(\backslash\%) = \frac{\mathrm{Weightofthedrugin the NLC}}{\mathrm{Weightofthedrugandnanocarrier}} \times 100\backslash\%$$

$$\mathrm{EE}\,(\backslash\%) = \frac{\mathrm{Weightofthedrugin the NLC}}{\mathrm{Weightofthedrugadded}} \times 100\backslash\%$$

2.3.2.3. Morphology of dasa-NLC

The morphology of dasa-NLC was captured by TEM. Briefly, dasa-NLC was diluted with purified water for 30 times and was subsequently deposited on a copper grid for 10 min. The excess fluid was drawn off with a filter paper and one drop of 1% phosphotungstic acid solution was deposited on the grid for 1.5 min. After the excess phosphotungstic acid solution was draw off, the copper grid was air-dried before being analyzed by TEM (Hitachi H-7650, Japan).

2.3.2.4. *In vitro* drug release

The *in vitro* release profile of dasa-NLC was assessed by a dialysis method as reported before(16). Briefly, 1 mL dasa-NLC was placed into a dialysis bag (MWCO = 3500) and was subsequently immersed in 100 mL of release medium (0.45% Tween 80 solution, 34 ± 0.5 °C) with a stirring speed of 200 rpm. At predetermined time intervals, 1 mL of the released samples were withdrawn and replaced by an equal

volume of the fresh release medium. The quantification of dasatinib in the samples was determined by HPLC and the cumulative release profile was plotted by using a GraphPad Prism software (Version 7.0, USA). Same amount of dasatinib solubilized in 15% propylene glycol (PEG) was chosen as a control. The experiments were carried out in triplicates.

2.3.3. Eye irritation test

A draize rabbit eye test was applied to evaluate possible ocular irritation of dasa-NLC. Briefly, 100 μL of dasa-NLC was instilled onto the cornea of the New Zealand albino rabbit 3 times a day for consecutive 7 days and the eyes were monitored every day for signs of discomfort. The eyes instilled with 100 μL dasatinib-PEG solution or normal saline were assigned as the positive control and negative control, respectively. The image of the eyes under natural light or the eyes applied with 2% fluorescein sodium solution followed by cobolt blue light illumination were captured.

2.3.4. *In vitro* angiogenesis related cell-based assay

2.3.4.1. Cell culture

Human umbilical vein endothelial cells (HUVEC) were cultured in DMEM/F12 medium with 10% FBS at 37 ℃ with 5% CO_2.

2.3.4.2. Anti-proliferation assay

The anti-proliferation effect of dasa-NLC was evaluated by an MTT assay. Briefly, HUVEC cells were seeded into a 96-well plate with a density of 5000 cells/well. After incubation for 24 hours, the cell culture medium was replaced by free dasatinib at its solubility or dasa-NLC with different concentrations. 72 hours later, an MTT assay was conducted to determine the percentage of proliferation relative to the control (no drug treatment).

2.3.4.3. Anti-migration assay

The anti-migration effect of dasa-NLC was assessed with a scratch injury assay as reported before with modifications(17). Briefly, HUVEC cells were seeded into a 6-well plate with a density of 6×10^5 cells/well. After incubation for 24 hours, HUVEC cell monolayers were scratched with a 200 μL pipette tip (5 scratched lines per well) and carefully washed with PBS for 3 times to remove the detached cells. Next, free dasatinib at its solubility or dasa-NLC with different concentrations was added. The experiment was undertaken in triplicate. The images of cells were captured before and after incubation for 18 hours and the migrated distance was quantified by an Image J software (NIH, USA).

2.3.4.4. Anti-tube formation assay

The anti-tube formation effect of dasa-NLC was evaluated with a method reported before with modifications(18). Briefly, Matrigel® Matrix was thawed at 4℃ overnight before being coated into a 96 well plate (50 μL/well) and the gel was solidified after being incubated in 37℃ for 30 min. Next, HUVEC cells pre-treated with free dasatinib at its solubility or dasa-NLC were seeded (6×10^4 cell/well) in the gel

coated-96 well plate. 8 hours later, the images of the cells in each well were captured by an inverted microscope (Nikon DS-Ri2).

2.3.5. *In vivo* anti-CNV assay

2.3.5.1. Mouse model of CNV

A mouse model of CNV was established by using an alkaline burned method as reported previously with modifications (19). Briefly, mice were anesthetized with an intraperitoneal injection of 4% chloral hydrate and one drop of tetracaine was subsequently applied on the surface of the right eye to provide local anesthesia. Next, a round piece of filter paper (2 mm diameter) soaked with 2.5 μL of NaOH solution (1 M) was placed onto the central cornea. 1 min later, the filter paper was removed and the cornea was rinsed extensively with 20 mL of sterile saline solution. A drop of normal saline or dasa-NLC at different concentrations (10 μL) was instilled on the surface of alkali-injured eyes three times a day for consecutive 14 days. The alkaline burned eyes instilled with saline were chosen as controls.

2.3.5.2. Observation and quantification of CNV

On day 3, day 7 and day 14 after the alkaline burn, the mice (6 mice/group/time point) were anesthetized with an intraperitoneal injection of 4% chloral hydrate and the pupil was dilated with a 0.5% tropicamide eye drop. Next, the eyes of the mice were examined by a dissecting microscope and the images of the eyes were captured with a camera (Nikon, Japan). The percentage of CNV covered area (A%) was quantified by the following formula:

$$\mathrm{A}\backslash\% = \frac{\mathrm{C}}{12} \times 3.14 \times \left[\mathrm{r}^2 - (\mathrm{r} - \mathrm{l})^2\right] \times 100\backslash\%$$

in which C represents the clock hours of CNV coverage in the cornea, l is the average length of the vessels sprouted at each clock hour, r is the diameter of the mouse cornea (1.5 mm).

2.3.5.3. Histological assessment of mouse eyes

Mice were euthanized on day 3, day 7 and day 14 after the alkaline burn. The eyes were inoculated and placed into a 4% paraformaldehyde solution at 4℃ overnight and followed by embedded in the paraffin after dehydration with an ethanol gradient. Sagittal sections (5 μm) were prepared and stained with hematoxylin and eosin (H&E). The image of the H&E stained cornea was captured by using a SOPTOP microscope (Sunny Optical thechnology co., LTD, China).

2.3.5.4. Immunohistochemical analysis

Immunohistochemical analysis of total Src and phospho-Src in the cornea was performed according to the manufacturer's instructions. Briefly, the specimens on the slides were deparaffinized in xylene and rehydrated with an ethanol gradient, followed by antigen retrieval in citrate buffer (pH 6.0). After being incubated in a 3% H_2O_2 solution for 25 min, the samples were washed with PBS for 3 times and were treated with blocking buffer (3% BSA) for 30 min. The specimens were subsequently incubated in primary

anti-Src rabbit polyclonal antibody or anti-Src phospho Y418 antibody overnight at 4 °C. Next, the specimens were treated with an HRP conjugated Goat Anti-mouse IgG (H + L) for 50 min at room temperature. After being washed by PBS for 3 times, the samples are treated with DAB solution and hematoxylin. The image of the cornea was captured by using a SOPTOP microscope.

2.3.6. Statistical Analysis

Results are presented as mean ± SD. One-way ANOVA with Tukey Kramer post-hoc test was used to compare differences among three or more groups. Data analyses were performed using SPSS (22.0, IBM, Armonk, NY, USA). $p < 0.05$ was considered to be statistically significant.

3. Results

3.1 Preparation and physicochemical characterization of dasa-NLC

NLC is one of the most promising ophthalmic drug delivery systems. We successfully encapsulated dasatinib into NLC via a melt-emulsification method and its physicochemical properties are summarized in Table 1 and Fig. 1. Dasa-NLC exhibited an average size of 78.53 nm with a narrow distribution (PDI = 0.21 ± 0.01). As the aqueous solubility of dasatinib was reported to be 0.4 μg/mL(20), the NLC improved its solubility by more than 1220x to about 488.57 μg/mL. The drug loading was 1.46%±0.01%, which was within the typical range of drug loading of NLC(13, 21–23). As indicated in the TEM image (Fig. 1a), dasa-NLC were spherical nanoparticles with an average size about 80 nm, which was consistent with the DLS measurements. In the *in vitro* drug release study (Fig. 1b), dasa-NLC exhibited a sustained release profile. Compared with the free drug that was quickly released out within 4 hours, dasa-NLC exhibited a much slower drug releasing rate with only 6.85% ± 5.92% dasatinib were released out from the NLC in 4 hours and 25.14% ± 10.57% dasatinib were released out in 24 hours (Fig. 1b).

Table 1
The physico-chemical properties of blank and drug-encapsulated NLC.

	Size (nm)	PDI	Zeta potential (mV)	Solubility (μg/ml)	EE%	DL%
Blank NLC	80.14 ± 1.95	0.23 ± 0.01	-28.0±-1.75	-	-	-
Dasa-NLC	78.53 ± 0.36	0.21 ± 0.01	-29.56±-1.00	488.57 ± 4.46	97.71% ±0.89%	1.46% ±0.01%
Coumarin 6-NLC	78.32 ± 0.54	0.21 ± 0.01	-29.25±-1.04	69.23 ± 3.34	-	-

3.2 Eye irritation test

No sign of discomfort or toxicity was observed for rabbits instilled with the dasa-NLC or normal saline for up to 7 days. The cornea of rabbits in these two groups remained clear and smooth (Fig. 2). By stark contrast, obvious signs of damaged cornea were noted in the dasatinib-PEG group. Conjunctiva edema was observed 1 hour after the eye was instilled with 1 drop of dasatinib-PEG solution (100 µL). On the second day, red swollen conjunctiva, large amount of thick eye discharge, opaque cornea and serious inflammatory response were developed, diffused fluorescence staining of the cornea could be observed under cobolt blue light, which indicated sever cornea and conjunctiva damage caused by the dasatinib-PEG solution (Fig. 2). On day 7, deformed conjunctiva and diffused fluorescence staining of the cornea remained to be obvious. While for the eyes administrated with blank PEG solutions, only minor edema in conjunctiva was noted 1 hour after the instillation, which was recovered in the second day, no presence of corneal fluorescence staining for up to 7 days. This result indicates that dasa-NLC up to a concentration of 488 µg/mL exhibited no acute ocular irritation, while dasatinib-PEG solution with an equal concentration of dasatinib resulted in severe ocular toxicity and the toxicity effect was due to high concentration of dasatinib instead of PEG.

3.3 *In vitro* anti-angiogenesis effect in cell-based assays

As proliferation, migration and tube formation are important pathological processes in the development of angiogenesis(5), the anti-angiogenesis effect of dasa-NLC was assessed by examining its anti-proliferation, anti-migration and anti-tube formation effect in HUVEC cells.

The anti-proliferation effect was evaluated with an MTT assay. As shown in Fig. 3a, free dasatinib at its saturated solubility inhibited the proliferation of HUVEC cells by approximately 26.82% ± 2.34%. Compared with free dasatinib, dasa-NLC significantly improved the anti-proliferative effect of dasatinib ($p < 0.05$) and exhibited a dose-dependent anti-proliferative effect. At 1 µM, dasa-NLC inhibited cell proliferation by about 38.26% ± 6.08% and at 25 µM, dasa-NLC inhibited cell proliferation by about 73.79% ± 5.78%.

A scratch injury assay was used to assess the anti-migration effect of dasa-NLC. The migration of HUVEC cells was quantified by measuring the migrated distance of the cells with an Image J software. As shown in Fig. 3b and Fig. 3c, for the cells without any treatment, a migrated distance of about 56.62 µm was observed after being incubated in 18 hours. While for the cells treated with free dasatinib at its saturated solubility or dasa-NLC, the migrated distance was significantly reduced. The migrated distance of the cell treated with dasa-NLC at 1 µM was 14.65 ± 5.35 µm which was not significant different from that of the cell treated with free dasatinib at its solubility (17.63 ± 3.43 µm). When the dasatinib concentration in NLC was increased to 5 µM and 25 µM, the migrated distance was 9.62 ± 0.62 µm and 10.27 ± 0.82 µm respectively, which are significant lower than that of the free dasatinib at its solubility.

The anti-tube formation effect of dasa-NLC was shown in Fig. 3d. For the control group (no drug treatment), extensive tubes were formed when the cells were incubated in the matrigel for 8 hours. However, for the cells pretreated with free dasatinib at its solubility or dasa-NLC (1 h), no signs of tube

formation were noted for a consecutive observation of 24 hours. Our results indicated that dasatinib exhibited a strong anti-tube formation effect even at a very low concentration (0.4 μg/mL, 0.82 μM) and when being encapsulated in NLC, the strong anti-tube formation effect was maintained.

3.4 Observation and quantification of CNV

To investigate the *in vivo* anti-CNV effects of dasa-NLC, an alkaline burned CNV model was established in mice. As indicated in Fig. 4, alkaline burn induced an obvious cornea angiogenesis. On day 3, the CNV covered area was 56.84% ± 3.91%, cornea edema could be observed, the blood vessels were thin and loosely distributed, some blood vessels even extended to the central cornea. On day 7, the CNV covered area was increased to 83.46% ± 12.87%, thick and densely distributed blood vessels, cornea edema and bleeding could be found. On day 14, the CNV covered area was 84.23% ± 18.41%, the cornea bleeding became extremely severe. When treated with dasa-NLC, the development of CNV was greatly inhibited. The CNV covered area were 38.56% ± 11.09% and 45.84% ± 3.65% for the eye treated with 485 μg/mL and 48.5 μg/mL dasa-NLC respectively on day 3, which were significantly lower than that of the control group. Similarly, the CNV covered area in these two groups was also significantly lower than that of the control group on day 7. While on day 14, only the group treated with 485 μg/mL dasa-NLC exhibited a significantly lower CNV covered area compared with the control group (56.14% ± 11.42% vs 84.23% ± 18.41%). Relatively loosely distributed vessels, no bleeding was also observed for this group at all time points. These results indicated that dasa-NLC could significantly inhibit the neovascularization in the cornea.

3.5 Histological observation

H&E stained corneal sections were evaluated to assess the structural difference in different groups. As shown in Fig. 5 and Fig. S3, normal cornea exhibited a uniform and clear structure with neatly arranged epithelial cells, regularly and orderly arrayed collagen fibers in the stroma. No vascular structure could be observed. While for the control group (alkaline burn with the treatment of normal saline), a significant decrease in corneal epithelium thickness, irregular arrangement of epithelial cells, thickened collagen fiber spaces and disordered collagen fiber arrangement in the stroma were observed in the central cornea and the appearance of CNV in the superficial stroma of the periphery cornea were noted on day 3. On day 7, the degree of central cornea edema was increased, large amount of inflammatory cell infiltration, CNV and red blood cells were found in the stroma of central cornea. On day 14, cornea edema was alleviated and a large amount of CNV and blood cells in the stroma could still be observed in the central cornea. When the alkaline burned eyes were treated with dasa-NLC, the thinned epithelial layer and thickened collagen fiber space was found in the central cornea, CNV and inflammatory cell infiltration were observed in the periphery cornea on day 3, which was similar with the control group, except the distinct less CNV in the peripheral cornea of the group treated with NLC in high dasatinib concentrations (485 and 48.5 μg/mL). On day 7, the drug treated eyes showed less swelled stroma and less blood cells compared to the control, especially for the eyes treated with 485 μg/mL dasa-NLC, which exhibited no blood cells in the central cornea. On day 14, reduced collagen fiber space, alleviated stroma edema was observed in

dasa-NLC treated eyes. In the eyes treated with 485 μg/mL dasa-NLC, the central cornea was quite similar to the normal cornea except the thinned epithelial cell layer.

3.6 Immunohistochemical analysis

As mentioned earlier, Src is a critical component in the angiogenic signal cascade, the expression and activation of Src in the cornea was investigated by an immunohistochemical analysis. Tyrosine 418, a highly conserved region in Src-family kinases, locates in the catalytic domain of Src and is one of the autophosphorylation sites. Full catalytic activity of Src requires phosphorylation of tyrosine 418(24). Thus, phospho Y418 was used as a marker for the activation of Src. As exhibited in Fig. 6 and Fig. S4, minimal Src expression and no Src activation (phosphorylation of Src, pSrc) were observed in normal healthy stroma. The alkaline burn upregulated the expression of Src and pSrc in the stroma. When treated with dasa-NLC, the upregulation of Src and pSrc were significantly inhibited, especially in the group treated with dasa-NLC at high dasatinib concentrations (485 μg/mL).

4. Discussion

As elucidated earlier, due to the Src kinase and PDGFR inhibiting capability, dasatinib is a potential candidate for CNV. However, the efficacy of a drug could be compromised a lot by various delivery challenges such as poor drug solubility, fast drug clearance and cornea barriers. Various technologies could be applied to improve the drug solubility. However, the concentration depended toxicity of dasatinib should be carefully avoided. A drug delivery system with sustained release profile can mitigate the toxicity. In this study, dasatinib was encapsulated in NLC, a drug delivery system well known for solubility enhancement, sustain release and good ocular biocompatibility(4, 12–14).

Initially, a previously reported melt-emulsification method(15) was used to prepare the dasa-NLC. The particle size of the prepared NLC was about 17.8 nm with a polydispersity of 0.251. However, it was quite unstable and precipitated in the second day. The instability of this NLC was due to the small absolute value of the zeta potential (-7 ~ -8 mV). As the zeta potential implies the strength of repulsion forces between particles, higher absolute value of the zeta potential indicates better anti-aggregation and stability of the nanoparticle. An absolute value of about 30 mV was considered to be sufficient to guarantee the stability of NLC.(4) As a well-known biocompatible surfactant with negative charges, soy lecithin was added to the formulation to increase the absolute value of zeta potential and improve the stability of NLC. As shown in Table S1, soy lecithin could greatly enhance the stability of the NLC as well as the particle size. When 20 mg soy lecithin was added, the particle size of NLC was increased to 74.18 nm with an average zeta potential of -23 mV (about 50% in -15 mV, 50% in -30 mV). No precipitation could be observed in the first two days and only minor amounts of precipitation was found on the third day, which indicates an improved stability of NLC and the amount of soy lecithin was not sufficient. Therefore, in Formulation 3, 30 mg soy lecithin was added, the particle size was increased to -80.14 nm and the zeta potential was decreased to -28 mV and no precipitation was observed for consecutive 7 days. Therefore, Formulation 3 was used for the preparation of dasa-NLC. As mentioned

earlier, the efficacy of dasatinib was greatly limited by its poor water solubility, when being encapsulated in NLC, 488.57 ± 4.46 μg/mL dasatinib could be encapsulated, which is more than 1220 times higher than its saturated solubility (0.4 μg/mL). Lots of studies indicates that nanoparticles coated with chitosan showed a prolonged corneal retention time due to the electronic attractions and hydrogen bonds formed between the positively charged chitosan and the negatively charged mucus in the precorneal area(15, 25–27). As the prolonged residence time in the precorneal area would improve the ocular bioavailability of a drug, we have also prepared a oligochitosan-NLC (Supported information S1). This nanoparticle also exhibited a good stability in an observation of 7 days (Table S1). However, in our pilot study, when oligochitosan-NLC was applied on the alkaline burned cornea of mice, a severe adhesion of upper and bottom eye lids was observed in the second day and the eye lids could only be separated by force. This may be related to the enhanced inflammatory reactions(28, 29) in the alkaline burned wounds caused by the oligochitosan, and the eyelids were adhered together by the dried eye discharge. Therefore, NLC without chitosan was used to encapsulate dasatinib in this study.

Ocular safety is always a major concern when developing ophthalmic drug delivery systems. Dasatinib was initially developed for chronic myelogenous Leukemia(9), the toxicity of the drug should never be neglected, especially in our case, the solubility of drug was greatly improved. Drug delivery systems that provide sustained drug release profiles would be highly desirable to minimize the amount of drug that is in direct contact with the cornea and therefore reduce its ocular toxicity. In our study, the release profile of dasatinib from NLC was examined by a dialysis method and only 6.85% ± 5.92% dasatinib were released out from dasa-NLC in the first 4 hours, while the dasatinib were almost released out for dasatinib-PEG solution group within a same period (Fig. 1b). Next, the ocular irritation effect of dasa-NLC was examined by a draize rabbit eye test, in which fluorescein sodium staining is used to evaluate the intactness of corneal epithelium and positive fluorescent staining represents the discontinuity and defects of the corneal epithelium. As indicated in Fig. 2, dasa-NLC exhibited good ocular biocompatibility when it was instilled in the eye for consecutive 7 days (100 μL, 3 times/day). While the eye instilled with only 100 μL of dasatinib-PEG solution with a same dasatinib concentration exhibited severe toxicity. To examine whether the toxicity of dasatinib-PEG solution was caused by the high dastinib concentration or PEG, the eye irritation test was also undertaken for blank PEG solution and only minor conjunctiva edema was found in day 1, which was diminished in the second day. The result indicates that high concentration of dasatinib (488 μg/mL) can cause significant ocular toxicity, and this ocular toxicity could be greatly mitigated when dasatinib was encapsulated in the NLC. This superior ocular safety of dasa-NLC may be related to the good biocompatibility and sustain release of NLC.

As mentioned earlier, the efficacy of therapeutic agent was greatly compromised by the short residence time on the ocular surface, therefore, formulations with enhanced cornea penetration effect were quite helpful in improving the therapeutic effect of drugs. Coumarin 6, a fluorescent dye with poor water solubility, was used as a surrogate for dasatinib to assess the ocular penetration profile of NLC due to the similar physicochemical properties of dasa-NLC and coumarin 6-NLC (Table 1). As exhibited in Fig. S1, in the eye instilled with coumarin 6-PEG solution, green fluorescence could only be observed in the pre-epithelium area in the first hour. However, for the eyes instilled with coumarin 6-NLC, green fluorescence

could be observed in the pre-epithelium area in the first two hours after the instillation and the fluorescent dye spread throughout the cornea in 4 hours after the instillation. Therefore, NLC could facilitate the penetration of loaded drug into the cornea, this may be related to the penetration enhancing effect of Gelucire 44/14(30).

To examine the anti-CNV effect of dasa-NLC, several angiogenesis related cell based assays such as proliferation, migration and tube formation were used. First of all, the cytotoxicity of dasa-NLC to HUVEC cells was examined to exclude the influence of cytotoxicity on other cell based assays. As shown in Fig. S2, dasa-NLC was not cytotoxic up to 25 μM as the viability of HUVEC cells was not significantly altered after being incubated with dasa-NLC. 25 μM was also the highest concentration used in other cell-based assays. As exhibited in Fig. 3, dasa-NLC significantly improved the anti-proliferation and anti-migration efficacy of dasatinib, which may be related to the enhanced solubility provided by NLC. Besides, free dasatinib exhibited an extremely strong anti-tube formation effect and dasa-NLC could maintain this anti-tube formation effect of free dasatinib.

An alkaline burned CNV mice model, a model widely used for assessing the anti-CNV efficacy of various therapeutics, was used to corroborate the *in vivo* efficacy of dasa-NLC. The eyes treated with dasa-NLC exhibited a significant smaller CNV covered area ratio especially for the eyes treated with dasa-NLC at 485 μM (Fig. 4). In the histology study, the eyes treated with dasa-NLC exhibited less stroma edema and less blood cells. Taken together, dasa-NLC could significantly inhibit the CNV.

As Src is a critical component in the signal cascade of angiogenesis inducement and development, the expression and activation of Src (pSrc) in the cornea with or without the treatment of dasa-NLC were also evaluated. In our study, alkaline burn could significantly increase the expression of Src and pSrc in the stroma (Fig. 6 and Fig. S4) and this may be related to the up-regulated growth factors and inflammatory response caused by the alkaline burn. Alkaline burn was reported to induce a dramatic up-regulation of IL-1β, IL-6, transforming growth factor β (TGF-β), CD34, CD31, VEGF *etc.* in the cornea(18, 19, 31). The cytokines could activate Src family kinase, which could in turn mediate the production of these cytokines(32). When the alkaline burned eyes were treated with dasa-NLC, both the expression of Src and pSrc were significantly lower than the control group, especially for the group of 485 μM dasatinib. Our results indicate that dasa-NLC could inhibit the upregulation of Src and pSrc in alkaline burned cornea.

5. Conclusions

In this study, dasa-NLC was successfully prepared with an enhanced solubility of more than 1220 times. It is a spherical shaped nanoparticle with an average particle size of 78.5 nm. Dasa-NLC could sustain drug release, enhance the penetration of dasatinib into the cornea and were not irritant to the eye. Compared with the free dasatinib, dasa-NLC significantly inhibited angiogenesis-related cellular changes, such as proliferation, migration and tube formation. In the *in vivo* alkaline burned CNV model, dasa-NLC significantly inhibited the CNV development, pathological changes of the cornea, the expression and

activation of Src family kinase. As a result, dasa-NLC exhibits great potential as a novel pharmacotherapy in the management of CNV.

Abbreviations

NLC	Nanostructured lipid carriers
CNV	Corneal neovascularization
PDGFR	Platelate derived growth factor receptor
VEGF	Vascular endothelial growth factor
bFGF	Basic Fibroblast growth factor
EGF	Epidermal growth factor
GMS	Glyceryl monostearate
PDI	Polydispersity index
EE	Encapsulation efficiency
DL	Drug loading
MWCO	Molecular weight cut off
TGF-β	transforming growth factor β

Declarations

Acknowledgments

We are grateful for the financial support from the National Science Foundation of Shanxi Province (2020JQ-093), the Project of Independent Innovative Experiment for Postgraduates in medicine in Xi'an Jiaotong University (YJSCX-2018-005) and National Natural Science Foundation of China (81973409, 81903733).

Authors' contributions

LQQ designed the experiments and wrote the manuscript. Yxw, Spr, Kxm, Wmh conducted the animal experiments. Zpp, Mf and Zjy revised the manuscript. All authors read and approved the final manuscript.

Availability of data and materials

The datasets used and/or analyzed during the current study are available from the corresponding author on reasonable request.

Ethics approval and consent to participate

Not applicable.

Consent for publication

Not applicable.

Competing of interest

None

References

1. Mukwaya A, Mirabelli P, Lennikov A, Thangavelu M, Jensen L, Peebo B, et al. Repeat Corneal Neovascularization is Characterized by More Aggressive Inflammation and Vessel Invasion Than in the Initial Phase. Invest Ophthalmol Vis Sci. 2019;60(8):2990–3001.
2. Sharif Z, Sharif W. Corneal neovascularization: updates on pathophysiology, investigations & management. romanian journal of ophthalmology. 2019;63(1):15–22.
3. Kim JW, Jeong H, Yang MS, Lim CW, Kim B. Therapeutic effects of zerumbone in an alkali-burned corneal wound healing model. Int Immunopharmacol. 2017;48:126–34.
4. Seyfoddin A, Shaw J, Al-Kassas R. Solid lipid nanoparticles for ocular drug delivery. Drug Deliv. 2010;17(7):467–89.
5. Bai Y, Bai L, Zhou J, Chen H, Zhang L. Sequential delivery of VEGF, FGF-2 and PDGF from the polymeric system enhance HUVECs angiogenesis in vitro and CAM angiogenesis. Cell Immunol. 2018;323:19–32.
6. Roshandel D, Eslani M, Baradaran-Rafii A, Cheung AY, Kurji K, Jabbehdari S, et al. Current and emerging therapies for corneal neovascularization. Ocul Surf. 2018;16(4):398–414.
7. Li P, Chen D, Cui Y, Zhang W, Weng J, Yu L, et al. Src Plays an Important Role in AGE-Induced Endothelial Cell Proliferation, Migration, and Tubulogenesis. Front Physiol. 2018;9:765.
8. Le XF, Bast RC. Jr. Src family kinases and paclitaxel sensitivity. Cancer Biol Ther. 2011;12(4):260–9.
9. Zeng XP, Wang LJ, Guo HL, He L, Bi YW, Xu ZL, et al. Dasatinib ameliorates chronic pancreatitis induced by caerulein via anti-fibrotic and anti-inflammatory mechanism. Pharmacol Res. 2019;147:104357.
10. Chan PS, Xian JW, Li Q, Chan CW, Leung SSY, To KKW. Biodegradable Thermosensitive PLGA-PEG-PLGA Polymer for Non-irritating and Sustained Ophthalmic Drug Delivery. AAPS J. 2019;21(4):59.
11. Hosoya K, Lee VH, Kim KJ. Roles of the conjunctiva in ocular drug delivery: a review of conjunctival transport mechanisms and their regulation. Eur J Pharm Biopharm. 2005;60(2):227–40.
12. Khames A, Khaleel MA, El-Badawy MF, El-Nezhawy AOH. Natamycin solid lipid nanoparticles - sustained ocular delivery system of higher corneal penetration against deep fungal keratitis: preparation and optimization. Int J Nanomed. 2019;14:2515–31.

13. Dumont C, Bourgeois S, Fessi H, Dugas PY, Jannin V. In-vitro evaluation of solid lipid nanoparticles: Ability to encapsulate, release and ensure effective protection of peptides in the gastrointestinal tract. Int J Pharm. 2019;565:409–18.
14. Sanchez-Lopez E, Espina M, Doktorovova S, Souto EB, Garcia ML. Lipid nanoparticles (SLN, NLC): Overcoming the anatomical and physiological barriers of the eye - Part II - Ocular drug-loaded lipid nanoparticles. Eur J Pharm Biopharm. 2017;110:58–69.
15. Li J, Liu D, Tan G, Zhao Z, Yang X, Pan W. A comparative study on the efficiency of chitosan-N-acetylcysteine, chitosan oligosaccharides or carboxymethyl chitosan surface modified nanostructured lipid carrier for ophthalmic delivery of curcumin. Carbohydr Polym. 2016;146:435–44.
16. Zhang P, Yang X, He Y, Chen Z, Liu B, Emesto CS, et al. Preparation, characterization and toxicity evaluation of amphotericin B loaded MPEG-PCL micelles and its application for buccal tablets. Appl Microbiol Biotechnol. 2017;101(19):7357–70.
17. Battaglia L, Gallarate M, Peira E, Chirio D, Solazzi I, Giordano SM, et al. Bevacizumab loaded solid lipid nanoparticles prepared by the coacervation technique: preliminary in vitro studies. Nanotechnology. 2015;26(25):255102.
18. Jiang N, Ma M, Li Y, Su T, Zhou XZ, Ye L, et al. The role of pirfenidone in alkali burn rat cornea. Int Immunopharmacol. 2018;64:78–85.
19. Tian Y, Li H, Liu X, Xie L, Huang Z, Li W, et al. Pharmacological Inhibition of Caspase-8 Suppresses Inflammation-Induced Angiogenesis in the Cornea. Biomolecules. 2020;10(2):210.
20. Li Q, Lai KL, Chan PS, Leung SC, Li HY, Fang Y, et al. Micellar delivery of dasatinib for the inhibition of pathologic cellular processes of the retinal pigment epithelium. Colloids Surf B. 2016;140:278–86.
21. Saedi A, Rostamizadeh K, Parsa M, Dalali N, Ahmadi N. Preparation and characterization of nanostructured lipid carriers as drug delivery system: Influence of liquid lipid types on loading and cytotoxicity. Chem Phys Lipids. 2018;216:65–72.
22. Shrivastava N, Khan S, Baboota S, Ali J. Fabrication and Characterization of Timolol Maleate and Brinzolamide Loaded Nanostructured Lipid Carrier System for Ocular Drug Delivery. Curr Drug Deliv. 2018;15(6):829–39.
23. Kar N, Chakraborty S, De AK, Ghosh S, Bera T. Development and evaluation of a cedrol-loaded nanostructured lipid carrier system for in vitro and in vivo susceptibilities of wild and drug resistant Leishmania donovani amastigotes. Eur J Pharm Sci. 2017;104:196–211.
24. Wu SS, Yamauchi K, Rozengurt E. Bombesin and angiotensin II rapidly stimulate Src phosphorylation at Tyr-418 in fibroblasts and intestinal epithelial cells through a PP2-insensitive pathway. Cell Signal. 2005;17(1):93–102.
25. Sandri G, Motta S, Bonferoni MC, Brocca P, Rossi S, Ferrari F, et al. Chitosan-coupled solid lipid nanoparticles: Tuning nanostructure and mucoadhesion. Eur J Pharm Biopharm. 2017;110:13–8.
26. Li J, Tan G, Cheng B, Liu D, Pan W. Transport mechanism of chitosan-N-acetylcysteine, chitosan oligosaccharides or carboxymethyl chitosan decorated coumarin-6 loaded nanostructured lipid

carriers across the rabbit ocular. Eur J Pharm Biopharm. 2017;120:89–97.
27. Eid HM, Elkomy MH, El Menshawe SF, Salem HF. Development, Optimization, and In Vitro/In Vivo Characterization of Enhanced Lipid Nanoparticles for Ocular Delivery of Ofloxacin: the Influence of Pegylation and Chitosan Coating. AAPS PharmSciTech. 2019;20(5):183.
28. Du LQ, Wu XY, Li MC, Wang SG, Pang KP. Effect of different biomedical membranes on alkali-burned cornea. Ophthalmic Res. 2008;40(6):282–90.
29. Shi C, Zhu Y, Ran X, Wang M, Su Y, Cheng T. Therapeutic potential of chitosan and its derivatives in regenerative medicine. J Surg Res. 2006;133(2):185–92.
30. Ross BP, Toth I. Gastrointestinal absorption of heparin by lipidization or coadministration with penetration enhancers. Curr Drug Deliv. 2005;2(3):277–87.
31. Chen L, Zhong J, Li S, Li W, Wang B, Deng Y, et al. The long-term effect of tacrolimus on alkali burn-induced corneal neovascularization and inflammation surpasses that of anti-vascular endothelial growth factor. Drug Des Devel Ther. 2018;12:2959–69.
32. Liu ST, Pham H, Pandol SJ, Ptasznik A. Src as the link between inflammation and cancer. Front Physiol. 2013;4:416.

Figures

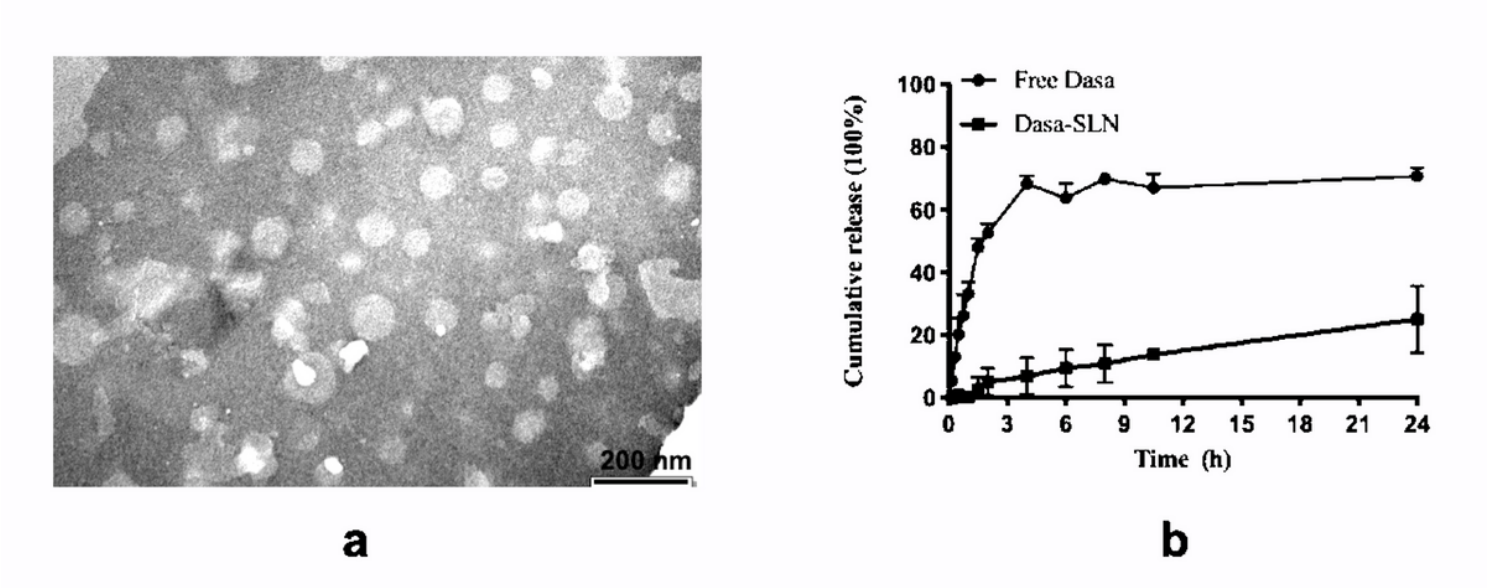

Figure 1

Physical characterization of dasa-NLC. a, the TEM image of dasa-NLC; b, in vitro release profile of dasa-NLC.

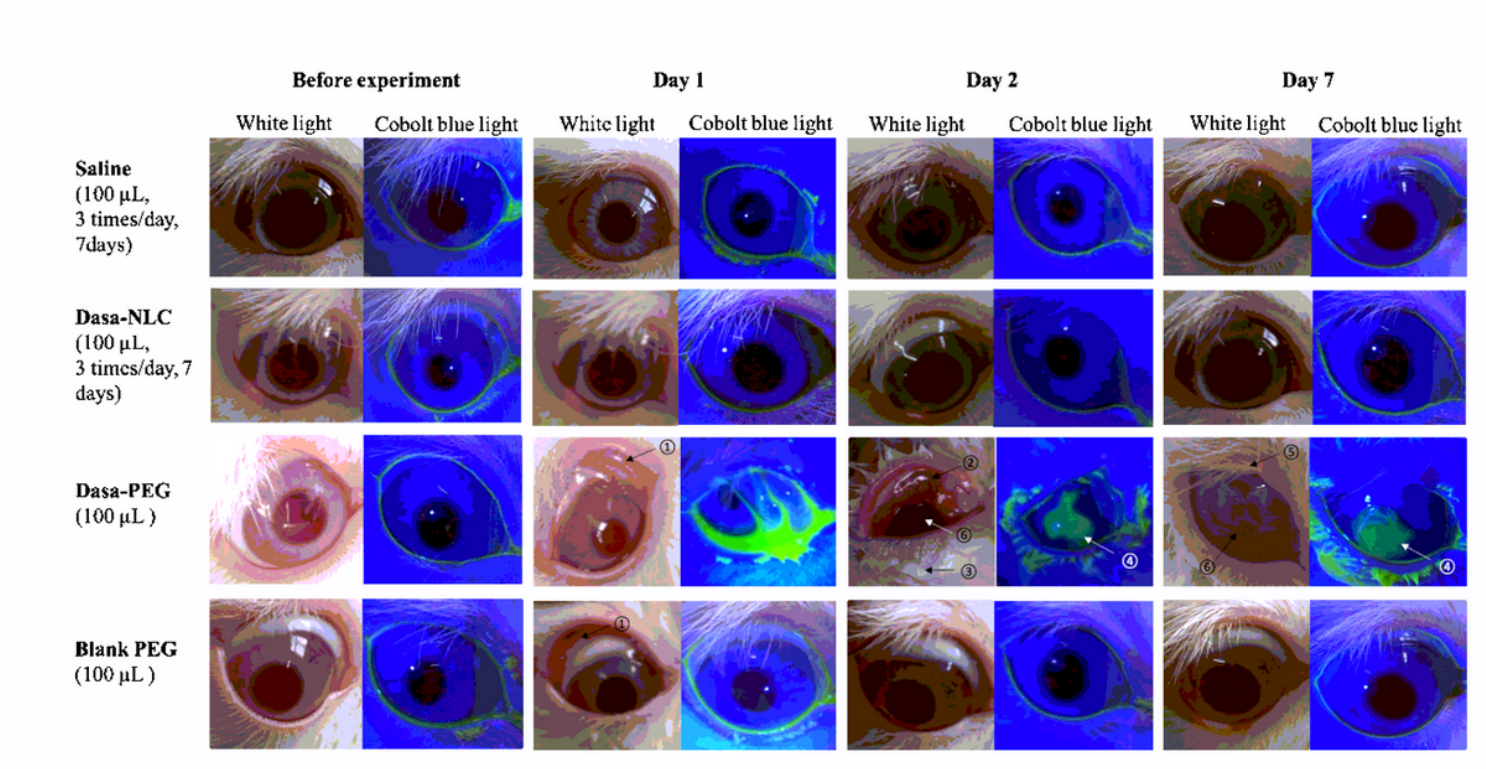

Figure 2

The ocular irritation test of dasa-NLC. ① conjunctiva edema, ② red swollen and inflammatory conjunctiva, ③ thick eye discharge, ④ diffused fluorescence staining of the cornea, ⑤ deformed conjunctiva, ⑥ opaque cornea.

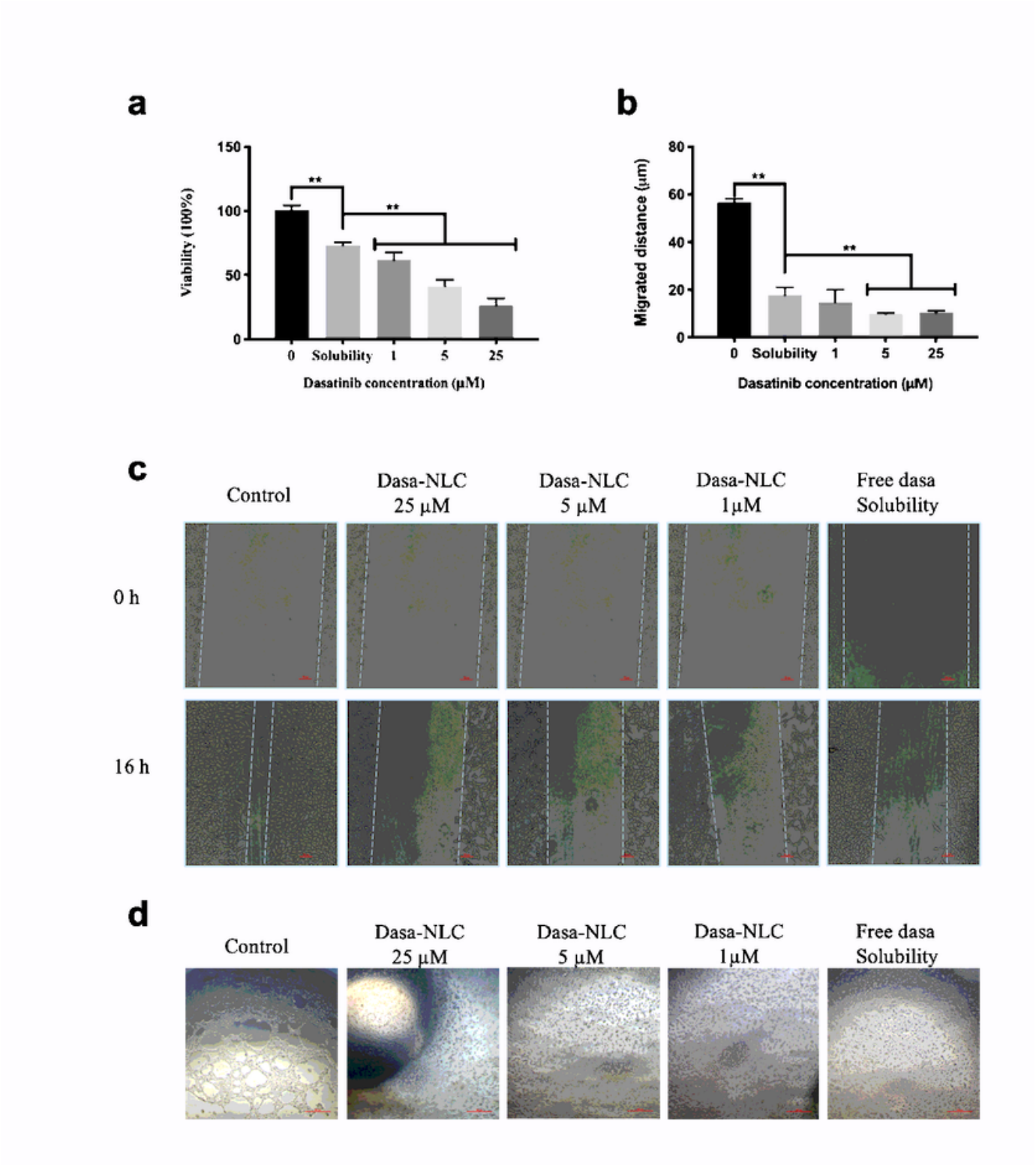

Figure 3

In vitro anti-angiogenesis effect of dasa-NLC. a: in vitro anti-proliferation effect of dasa-NLC, b: in vitro anti-migration effect of dasa-NLC, c: migration images of HUVEC cells with different treatments, d: in vitro anti-tube formation effect of dasa-NLC. * $p < 0.05$

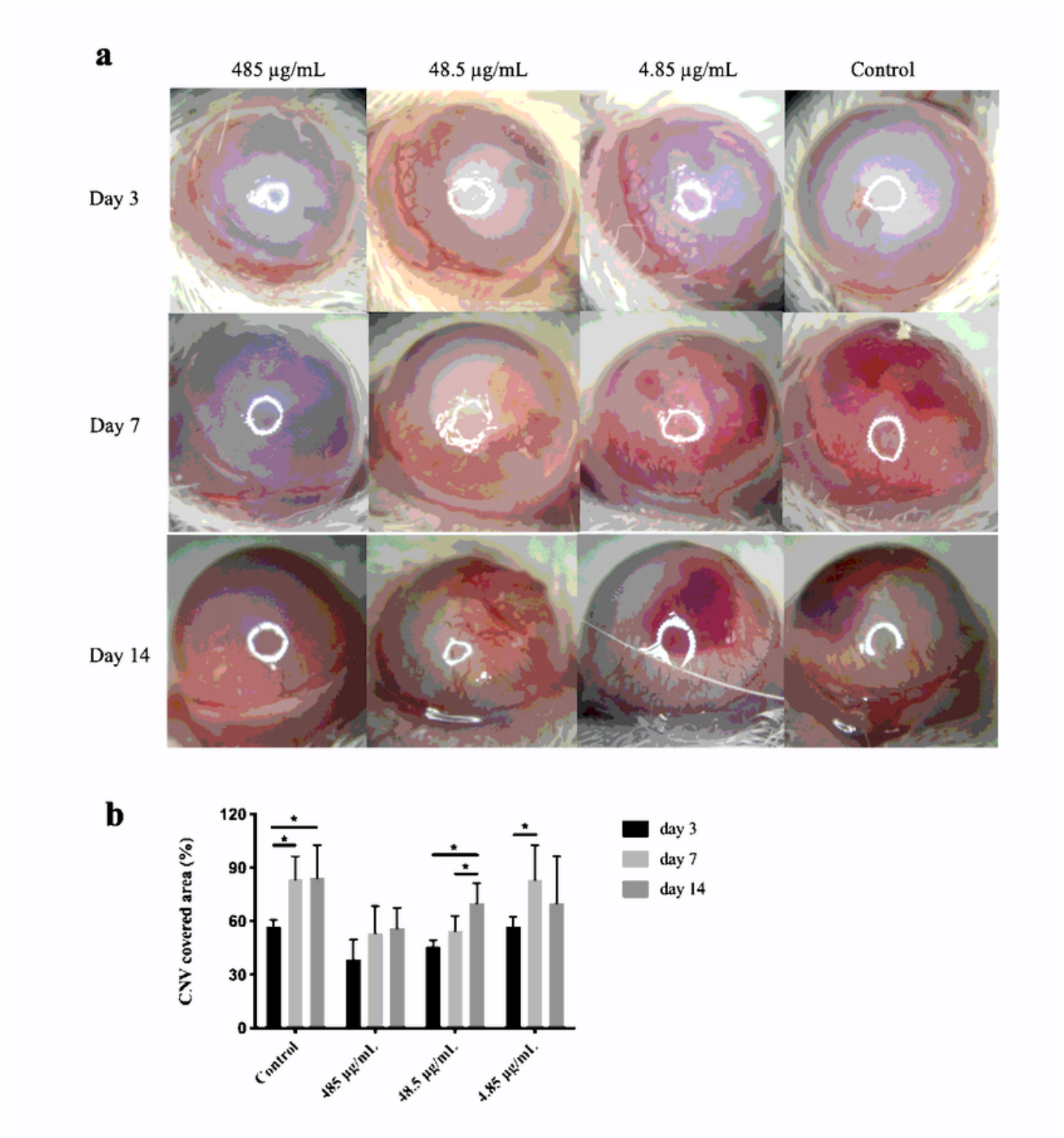

Figure 4

Pharmacological inhibition of CNV after corneal alkaline burn. a: images of the macroscopic CNV appearance after different treatments for different periods, b: statistical analysis of the CNV covered area after different treatments for different periods. * p <0.05.

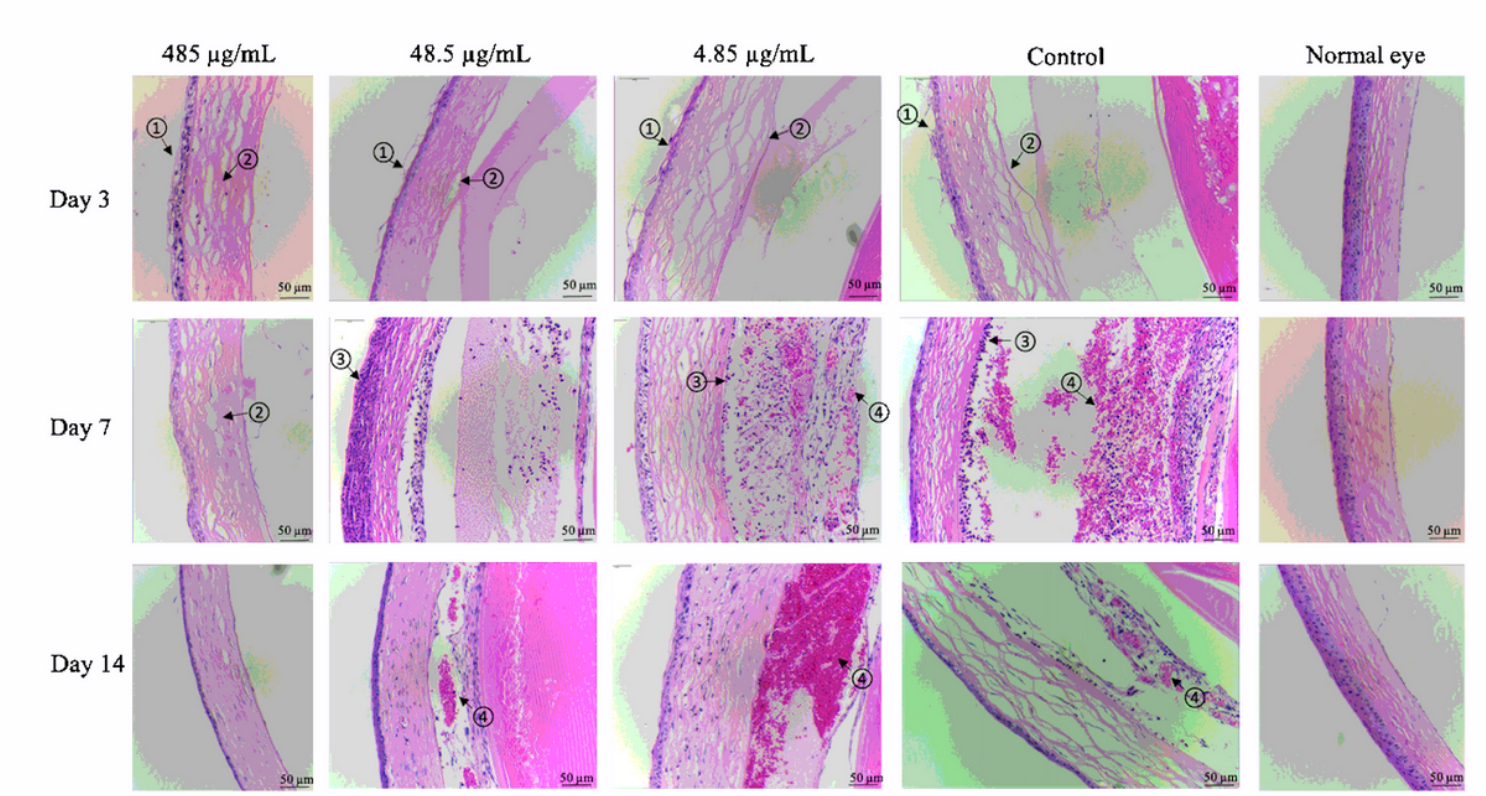

Figure 5

H&E staining of the central cornea from different groups for different periods. ① decreased corneal epithelial thickness, ② thickened collagen fiber space, ③ inflammatory cell infiltration, ④ blood cells.

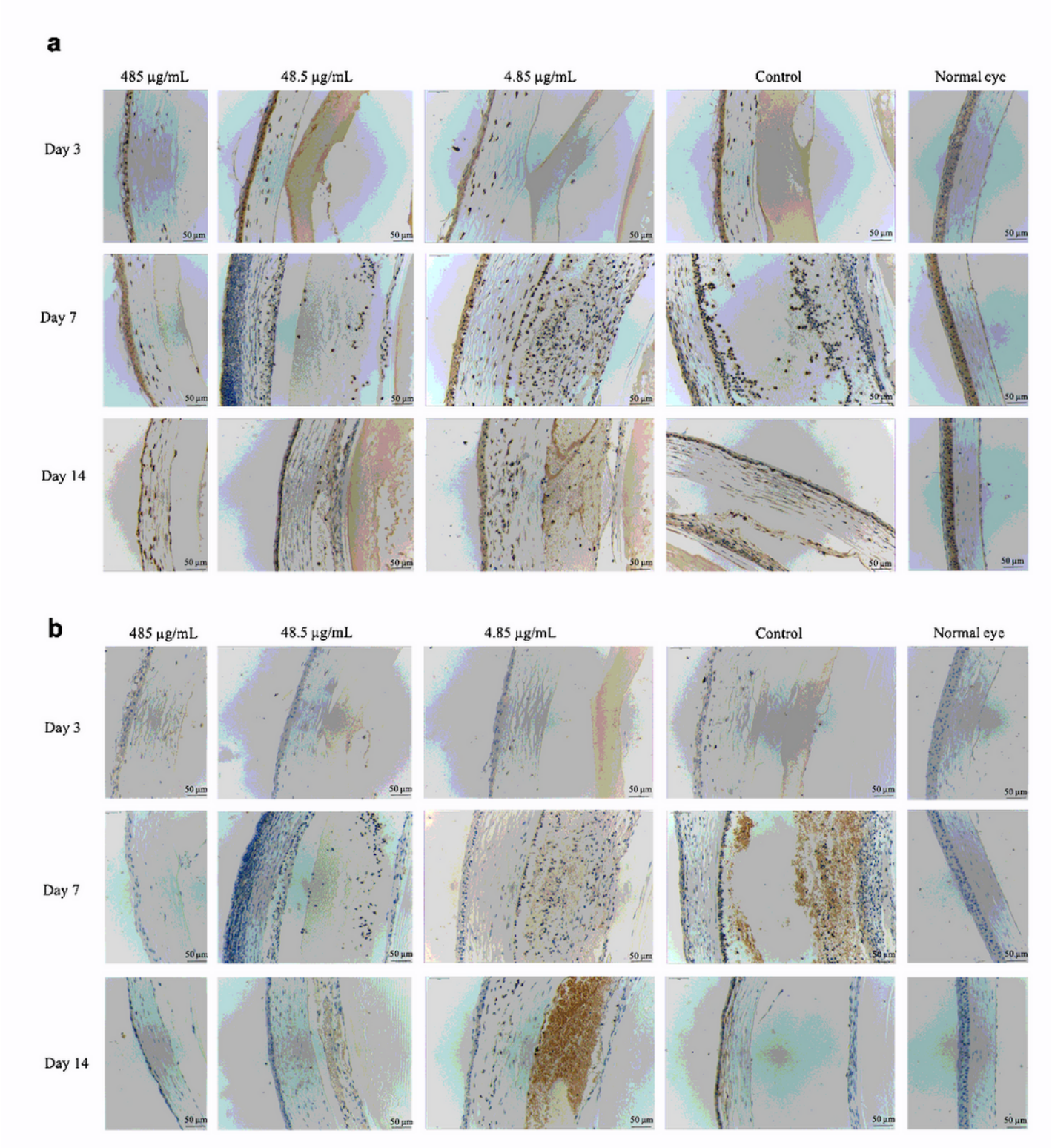

Figure 6

Immunohistochemistry staining of Src (a) and pSrc (b) in the central cornea with different treatments for different periods.

Supplementary Files

This is a list of supplementary files associated with this preprint. Click to download.

- Supplementarymaterial.docx